Cleaved CD95L perturbs in vitro macrophages responses to Toxoplasma gondii.

TIFFNEY, E.A., COOMBES, J.L., LEGEMBRE, P. and FLYNN, R.J.

2022

Short communication

Title: Cleaved CD95L perturbs *in vitro* macrophages responses to *Toxoplasma gondii*

Authors: Ellen A. Tiffney[1], Janine L. Coombes[1], Patrick Legembre[2], Robin J Flynn[1,3]*

Addresses:

[1] Dept. Infection Biology, Institute of Infection and Global Health, University of Liverpool, L3 5RF,

[2] Centre Eugène Marquis, Université Rennes-1, INSERM U1242, Rennes, France.

[3] Graduate Studies Office, Department of Research, Innovation and Graduate Studies, Waterford Institute of Technology, Ireland, X91 K0EK.

Correspondence *Robin J Flynn, Graduate Studies Office, Department of Research, Innovation and Graduate Studies, Waterford Institute of Technology, Cork Road, Ireland, X91 K0EK. robin.flynn@wit.ie, Tel +353 (0) 85 862 2662, Fax +353 (0) 51 30 2000.

Abstract

Toxoplasma gondii infects approximately 1-2 billion people, and manipulation of the macrophage response is critical to host and parasite survival. A cleaved (cl)-CD95L form can promote cellular migration and we have previously shown that cl-CD95L aggravates inflammation and pathology in systemic lupus erythematosus (SLE). Findings have shown that CD95L is upregulated during human infection, therefore we examined the effect of cl-CD95L on the macrophage response to *T. gondii*. . We find that cl-CD95L promotes parasite replication in macrophages, associated with increased arginase-1 levels, mediated by signal transducer and activator of transcription (STAT)6. Inhibition of both arginase-1 and STAT6 reversed the effects of cl-CD95L. Phospho-kinase array showed that cl-CD95L alters Janus Kinases (JAK)/STAT, mammalian target of rapamycin (mTOR), and Src kinase signals. By triggering changes in JAK/STAT cl-CD95L may limit anti-parasite effectors.

Keywords: *Toxoplasma gondii*; macrophage; CD95L; FasL; JAK/STAT; arginase; cleaved CD95L

1. Introduction.

Toxoplasma gondii is an obligate intracellular parasite capable of causing significant disease in both human and animal hosts. *T. gondii* has the ability to infect multiple cell types but preferentially infects monocytes or dendritic cells (DCs). Within these cells *T. gondii* is effectively able to control the host cell niche. Studies have demonstrated that parasite secreted effectors alter macrophage functions and their regulating signalling mechanisms [1]. Indeed, multiple effectors target the JAK-STAT cascade and confer virulence in recombinant avirulent strains of parasite [2]. This is a two-sided process, host priming of the macrophage is key to effective parasite control and incorrect priming, resulting in arginase-1 producing macrophage, cannot restrain parasite replication [3].

The CD95-CD95L (also known as Fas-FasL, respectively) interaction is key to controlling intracellular parasites via induction of cellular apoptosis [4]. Indeed, appropriate CD95 signalling post-infection is thought to control immunopathology [5]. Studies [6] have shown that *T. gondii* can inhibit CD95 mediated killing by impairing the correct functioning of caspase 8. Recently, CD95L has been shown to undergo a metalloprotease-mediated cleavage event leading to a ,soluble, cl-CD95L that drives cellular migration rather than death [4]. Additionally, we have recently shown that cl-CD95L causes exacerbated pathology during the onset of murine lupus due to increased cellular infiltration within inflamed tissues [7]. A previous survey of pregnant human toxoplasmosis patients had shown that this form of CD95L increased during chronic infection [8] and *in vitro* infection with *T. gondii* RH induced high levels of soluble cl-CD95L in both macrophages and trophoblast cells [9].

Given these findings we sought to directly assess the effect of soluble cl-CD95L on the outcome of macrophage infection with *T. gondii*. We report that cl-CD95L leads to increased

53 parasite replication partially dependent on changes in IL-6 and arginase-1 levels.
54 Interestingly, these opposing mechanisms may be explained by the finding that cl-CD95L
55 reprograms macrophages to acquire a Myeloid-Derived Suppressor Cell (MDSC)-like
56 phenotype.

57

2. **Methods**

2.1 Parasite Culture.

Host VERO cells were cultured in DMEM supplemented with 5% fetal bovine serum (FBS, F4135 Sigma Aldrich), penicillin-streptomycin (10,000 U penicillin & 100 mg/ml streptomycin (Sigma Aldrich) at 5% CO_2 at 37°C in 25 cm^2 flasks until cells were 80% confluent. The RH strain of *T. gondii* was used throughout the work. Parasites were propagated as tachyzoites by serial passage in VERO cells. For the purification of *T. gondii* tachyzoites, infected host VERO cells were dislodged from culture flasks by scrapping with a single-use rubber cell scraper. Dislodged cells were passed, through a sterile blunt-ended needle. Lysed cells and isolated parasites were centrifuged at 2,000 rpm for 10 minutes at room temperature (RT). Parasites were resuspended in 5 mL 1X D-PBS and this solution was added to a PD-10 column, columns were then washed with 5 mL 1X D-PBS. The number of parasites recovered was counted in 10 µL of parasite solution. Finally, the parasites were centrifuged for 10 minutes at 2,000 rpm, supernatant removed and resuspended in complete DMEM.

2.2 Bone marrow-derived macrophages (BMDM).

Bone marrow-derived macrophages were obtained from healthy wild-type C57BI/6 mice aged between 8-16 weeks. Animals were culled by standard schedule 1 procedures of exposure to rising concentrations of CO_2. Immediately afterwards hind femurs were removed and placed into sterile D-PBS for transport to the laboratory. Excess fat, muscle, and skin were removed. Thereafter, the bone marrow was flushed from the femur by repeated injecting, using a 2 mL syringe and a 25-gauge needle, of the femur with complete media. Cells were passed through a 70 µm cell strainer and centrifuged for 10 minutes at

1,500 rpm. Bone marrow cells were seeded at $2x10^6$/mL in a 6 mL petri dish with the addition of 20 ng/mL of M-CSF (Recombinant Murine M-CSF, PeproTech). Every two days the media and M-CSF was replenished until cells were harvested on day 7. Thereafter macrophages were seeded in 96 well flat-bottomed plates (Greiner Bio-One) at $2x10^4$/well. In some experiments chemical inhbitors or antibodies were added to cultures prior to infection as follows; anti-mouse IL-6 (BioXCell Clone MP5-20F3) was used at 120 ng/mL; to inhibit Arginase, N^{ω}-hydroxy-nor-Arginine (nor-NOHA) (Sigma) was used at 5 mM; to inhibit cl-CD95L, mFas-Fc Chimera (R&D Systems Cat No. 435-FA) was added at 200 ng/mL; and to inhibit STAT6, the compound AS1517499 (Sigma) was used at 0.2 mg/mL.

2.3 Percentage monolayer destruction and free parasite counts

VERO cells or BMDM were seeded into 24 well plates at $2.5x10^4$/well and incubated for 24 hours. Thereafter, cells were stimulated with cl-CD95L at indicated doses and 24 hours later cells were infected with *T. gondii* at $1x10^5$/well (MOI 4). After 3 hours the medium was changed to remove free extracellular parasites and replaced with fresh media. Thereafter, cells were incubated for 72 hours.After 72 hours post-infection the percentage of the VERO monolayer that has been destroyed was estimated using an Olympus BH2 microscope at X10 magnification, using a previously described method [10]. In brief, a counting grid was overlaid onto images and consistent squares were counted across images. Destruction was recorded were 50% of cells within a grid square no longer had an intact membrane. An aliquot of supernatant was used to determine the extracellular parasite load.

2.4 ATP and Cytokine Detection

Supernatants were collected from BMDM cultures and used for CellTiter-Glo assays for the detection of ATP. 100 µL of each sample and media controls, as background controls, were added to a 96-well opaque plate. The plate was then left at RT for 30 minutes to equilibrate. Thereafter, 100 µL of CellTiter-Glo® Reagent was added to each well. The contents were then mixed for 2 minutes on an orbital shaker, followed by a 10 minutes incubation at RT. Luminescence was then recorded using a luminometer. Cytokine ELISAs for IL-6 and IL-1β were conducted using commercially available kits from Invitrogen (Cat no. 88-7064-88, 88-7013, respectively).

2.5 Arginase assay.

Cell lysates were prepared in Triton X-100. 50 µL of 10 mM $MnCl_2$/50 mM Tris-HCl buffer (pH 7.5) and 50 µL of lysate were mixed and incubated for 10 minutes at 55^{o}C for enzyme activation. 50 µL of 0.5 M L-arginine substrate (pH 9.7) was added to the activated lysate and incubated for 1 hour at 37^{o}C. To stop the reaction the acid-stop solution that was comprised of H_2SO_4 (96%), H_3PO_4 (85%), and H_2O in a ratio of 1:3:7 was added to the samples. Finally, 9% isonitrosopriopherone was added to develop colour. The sample was then heated to 103°C for 45 minutes and allowed to cool in darkness for another 10 minutes. 200 µL aliquots are then added to a 96 well ELISA plate and absorbance measured at 540 nm.

2.6 BMDM Phospho-Kinase Array

To determine a global signalling profile a Phospho-Kinase Array Proteome Profiler was used (R&D Systems, Cat No. ARY003B) BMDM were either left unstimulated or stimulated with 100 ng/mL of cl-CD95L for 24 hours, after which macrophages were rinsed with D-PBS.

Macrophages were then solubilised at $1x10^7$ cells/mL in Lysis Buffer 6 (R&D systems). Samples were pipetted up and down in order to resuspend macrophages and incubated for 30 minutes at 2-8^oC. Samples were then microcentrifuged and the supernatant transferred to an Eppendorf tube. Membranes were placed in the wells of an 8-Well Multi-dish and filled with 1.0 mL of Assay Buffer 1, which served as a blocking buffer. The plate was incubated on a rocking platform shaker for 1 hour. Membranes were then washed in 20 mL of wash buffer. After which, 1.0 mL of prepared samples were added to both parts A and B of each membrane. The plate was then incubated on a rocking platform shaker overnight at 2-8^oC. Then 1.0 mL of reconstituted Detection Antibody Cocktail in Assay Buffer was added to each well and incubated with shaking for 1 hour at RT. After, 1.0 mL of diluted Steptavidin-HRP in Array Buffer 2/3 was added to each well of the plate and incubated with shaking for 30 minutes at RT. Membranes were then washed. After washing, 1.0 mL of Chemi-Reagent Mix was added to each membrane and incubated for 1 minute. After incubation, excess Chemi-Reagent Mix was removed from each membrane. Membranes were imaged using a ChemiDoc. Pixel Density was measured using ImageJ software. The pixel density was normalised to total protein concentration in each lysate as determined by BCA assay.

2.7 Statistics

Raw data was collected on Microsoft Excel workbooks. All data analysis was conducted using Prism 7 (GraphPad). P values of < 0.05 were taken as significant, thedetails of individual tests are reported in the figure legends.

3. Results

3.1 Cleaved-CD95L alters T. gondii replication within host cells.

We initially tested the effect of pre-treatment of the VERO cell line with cl-CD95L prior to infection with *T. gondii.* Infection with *T. gondii* alone increases cellular destruction from 2% in uninfected/unstimulated to 14% in infected/unstimulated (Fig.1A; $P < 0.01$). VERO cells were stimulated with 100 ng/mL of cl-CD95L and then infected with *T. gondii*, giving rise to 26% cellular destruction that is statistically significant compared with stimulated but uninfected cells (Fig. 1A; $P < 0.01$). The difference in cellular destruction between infected cultures when cl-CD95L was present was also statistically significantly different, $P < 0.01$ (Fig. 1A). Host cell destruction is often an indicator of cell egress. The number of parasites in the supernatant was determined after 48 hours of infection by manual counting. Figure 1B demonstrates that a significant increase in parasite replication occurs after stimulation with cl-CD95L ($12x10^4$/mL parasites) when compared to unstimulated VERO cells ($9x10^4$/mL parasites; P value <0.05). Having demonstrated that the increase in monolayer destruction above might be caused by the increase in *T. gondii* load following cl-CD95L stimulation we sought to determine if cl-CD95L was causing these effects by decreasing cell viability. We assessed extracellular ATP in supernatants, the results show that before infection, as expected, there are high levels of cell viability as indicated by high levels of ATP (Fig.1C). In comparison, after infection with *T. gondii* the levels of cell viability, in both unstimulated and stimulated conditions decrease (P value <0.001).

To ensure our results were representative of primary host cells, we assessed the effect of cl-CD95L in murine macrophages. Bone marrow derived macrophages (BMDMs) were matured from bone marrow in the presence of M-CSF for 7 days prior to collection and further use.

We investigated the impact of stimulation with cl-CD95L on parasite replication in BMDM by preforming parasite counts after 48 hours of infection. As shown Figure 1D, a significant increase in parasite counts occur after BMDM cultures have been stimulated with cl-CD95L when compared to unstimulated cultures (P value <0.05). Additionally, we demonstrated that the effects observed were directly due to cl-CD95L by use of a Fas-Fc fusion protein to compete with cl-CD95L [7]. Figure 1E demonstrates that in the presence of the decoy receptor CD95-Fc, parasite replication levels were not significantly different from untreated infected controls.

3.2 cl-CD95L alters arginase-1 and IL-6 levels during T. gondii infection.

To determine if the increase in parasite load, mediated by cl-CD95L, paralleled changes in the BMDM response to infection we measured IL-6 in the supernatants of infected BMDMs in presence or absence of cl-CD95L. Figure 2A clearly demonstrates that cl-CD95L treatment alone did not drive the increase in IL-6 alone but did elicit an increase in IL-6 in combination with *T. gondii* driven cytokine expression. IL-6 production driven in this manner was not anti-parasitic. Neutralisation of IL-6 in the presence or absence of cl-CD95L caused a decrease in parasite numbers (Fig.2B). As previously demonstrated cl-CD95L caused an increase in parasite number but this was reversed in the presence of anti-IL-6 (Fig.2B).

This led us to speculate that a second host factor, triggered by cl-CD95L, was responsible for the effects on parasite load in BMDMs. To test this, we first assayed cl-CD95L treated and infected BMDMs for arginase and found elevated levels following *T. gondii* infection but treatment with cl-CD95L resulted in a further increase in these levels (Fig.2D). Indeed, the effects of cl-CD95L induced increased arginase could be reversed with the application of the

inhibitor nor-NOHA. Simultaneous application of both cl-CD95L and nor-NOHA resulted in significant decrease in parasite levels compared with cl-CD95L treatment only (Fig.2D); levels of parasite obtained in cl-CD95L/nor-NOHA cultures were similar to those in non-treated infected controls (Fig.2D). Interestingly, we found arginase-1 and IL-6 to be mechanistically linked as nor-NOHA inhibition of arginase also caused a decrease in IL-6 levels during cl-CD95L stimulation and infection (Supplementary Fig.1). STAT6 is a major transcriptional regulatory of alternative activation of macrophages during helminth infection [11-13]. It has been shown to drive the expression of arginase-1 during both cytokine and pathogen stimulation. We employed chemical inhibition of STAT6 to determine if it was directing cl-CD95L mediated arginase. During stimulation alone, cl-CD95L caused an increase in arginase-1 activity (Fig.2F) but the application of a STAT6 inhibitor AS157499 caused a decrease in these levels. Importantly following infection, we found that the synergistic increase in arginase was also ablated (Fig.2F). Phenotypically inhibition of STAT6 gave rise to a lower number of parasites but only after the application of cl-CD95L (Fig.2G; $P<0.01$); suggesting that cl-CD95L drives a STAT6 response, upregulating arginase, that mediates reduced parasite killing. Our data above would indicate that IL-6 when induced by cl-CD95L is not protective; to test if cl-CD95L:STAT6 signalling is involving in this we assayed supernatants for IL-6 levels. We show that cl-CD95L drives a synergistic increase in IL-6 following *T. gondii* infection ($P<0.05$) and importantly STAT6 inhibition in this setting causes a complete removal of IL-6 (Figure 2H).

3.3 cl-CD95L modifies the macrophage signalling landscape.

To address whether there was a pattern of cell signalling induced by cl-CD95L that could underlie the effect on increased parasite replication, and associated immune responses in

BMDMs, we performed a Phospho-kinase profiler array on cl-CD95L stimulated BMDMs. Exploring the cellular environment preceding infection was important and thus our experimental design relied upon prior stimulation with cl-CD95L, as we had shown above that this resulted in a cellular environment more permissive to parasite replication. 38 of 43 kinases were found to be expressed under both stimulated and unstimulated conditions. Using a Log2 fold change we identified 23 kinases upregulated in stimulated vs unstimulated BMDMs (Fig.3A). These were subject to STRING (V11.0) analysis to identify potential interactions using a database search. The top five Biological Processes and Reactomes are depicted in Figure 3B. Not unexpectedly, 3 GO terms identified map to phosphorylation/signal transduction and one to apoptotic processes. Cytokine signalling and immune system responses were identified within the Reactome analysis.

A network was constructed from the log2 fold upregulated proteins and three nodes are apparent – one involving STATs, one centred on mTOR, and a third involving the Src family (Yes, Fyn, Lck). Multiple members of these nodes, including Yes/Fyn/Lck, have significant overlap with factors previously identified as being elicited by cl-CD95L [4, 7]. STAT2/3/5A were identified in a node; STAT2 was previously shown to be negatively regulation immune protection in *T. gondii* infection, as $STAT2^{-/-}$ macrophages more effectively control their parasite load [14]; while STAT3 mediates susceptibility to *T. gondii* [15, 16]; and STAT5 has been implicated, albeit weakly, with increased parasite susceptibility [17].

The node centred on mTOR may indicate an MDSC-like response to cl-CD95L stimulation. A role for MDSCs, and similar cells, have been subject to increasing scrutiny in the context of parasite immunity [18]. Given the heterogeneous nature of their surface marker profile [18], they may have potentially been incorporated into analysis of $Gr1^{+}$ monocyte populations in

prior *T. gondii* studies [19-22] as many of these $Gr1^+$ monocytes were also $CD11b^+$. Indeed a population corresponding to these cells was shown to exert both an anti-inflammatory effect during infection and immune hyporesponsiveness during acute *T. gondii* infection [22].

4. Discussion:

Increased levels of soluble CD95L have been found in both human toxoplasmosis and murine macrophage infection. Given its potential effects outside of triggering cell death we examined the effects of cl-CD95L on macrophage infection. Our findings lead us to conclude that exposure of host cells to cl-CD95L leads to increased *T. gondii* replication and a parallel rise in host cell destruction. Furthermore, this cell destruction is dependent on parasite replication but not CD95L apoptotic effects as noted by our ATP findings. We determined that IL-6 was also upregulated following cl-CD95L stimulated and *T. gondii* infection but this was not protective as indicated by neutralising antibody. This finding is in line with previous studies which also detail a role for IL-6 in promoting parasite intracellular replication [23] conflicting with the protective role also assigned to IL-6 [24]. This contradictory nature of the resulting macrophage population we obtained following cl-CD95L stimulation and *T. gondii* infection reflects a previous finding that duality in the macrophage population can exist. Arginase-1 has been widely reported to negatively impact upon immunity to intracellular parasites [3] and this is known to arise from a key role in driving alternative activation of macrophages[25]. Yap and colleagues have described a both classically and alternatively activated macrophages existing within the same pool of cells following *T. gondii* infection [26].

Combined, the data would suggest cl-CD95L drives STAT6 mediated expression of arginase-1 and IL-6; these factors may synergise with *T. gondii* infection to remove the protective effects of IL-6 and increase the susceptibility of host cells in an arginase-dependent fashion. This is consistent with prior reports of IL-6 acting to enhance alternative activation of macrophages in a STAT3 dependent fashion [27]. Importantly, the autocrine/paracrine

induction of arginase-1 by IL-6, via STAT3, has also been shown during Mycobacteria infection of macrophages [28]. Our Phosopho-kinase array data revealed that STAT6 was only one of multiple STAT members changed by cl-CD95L. Thus, here we show that the actions of cl-CD95L in promoting parasite replication stem from STAT6 they may, at least partially, from wider STAT signalling. Myeloid-derived suppressor cells have been linked to both suppressing but also promoting inflammation in a variety of setting including systemic lupus erythematosus (SLE) [29]; in this setting MDSCs expressing arginase-1 promoted Th17-mediated kidney damage. This endstage pathology overlaps with our previous finding that cl-CD95L drives selective recruitment of Th17 cells into tissues including in a murine model of SLE [7]. A potential outcome of cl-CD95L stimulation of macrophages could be the induction of an MDSC-like phenotype, independent of parasite infection. This is in part supported by the finding that mTOR is upregulated as are a number of other kinases associated with the MDSC phenotype. Our findings point to the need to closely examine the role of cl-CD95L during *T. gondii* pathogenesis *in vivo* and to define the role it plays in eliciting MDSCs. Specifically, does cl-CD95L elicit differentiation and trafficking of MDSCs and what role do these cells play *in vivo*.

Conflict of Interest: RJF and PL are applicants on a patent surrounding the use of CD95 therapeutics.

Acknowledgments: We would like to thank Catherine Hartley for her technical assistance and the staff at University of Liverpool Biomedical Services Unit. EAT was supported in part through a Wellcome Trust ISSF award to RJF.

References

[1] Jensen KD, Wang Y, Wojno ED, Shastri AJ, Hu K, Cornel L, et al. Toxoplasma polymorphic effectors determine macrophage polarization and intestinal inflammation. Cell Host Microbe 2011;9:472-83.
[2] Saeij JP, Coller S, Boyle JP, Jerome ME, White MW, Boothroyd JC. Toxoplasma co-opts host gene expression by injection of a polymorphic kinase homologue. Nature 2007;445:324-7.
[3] El Kasmi KC, Qualls JE, Pesce JT, Smith AM, Thompson RW, Henao-Tamayo M, et al. Toll-like receptor-induced arginase 1 in macrophages thwarts effective immunity against intracellular pathogens. Nat Immunol 2008;9:1399-406.
[4] Tauzin S, Chaigne-Delalande B, Selva E, Khadra N, Daburon S, Contin-Bordes C, et al. The naturally processed CD95L elicits a c-yes/calcium/PI3K-driven cell migration pathway. PLoS Biol 2011;9:e1001090.
[5] Hu MS, Schwartzman JD, Yeaman GR, Collins J, Seguin R, Khan IA, et al. Fas-FasL interaction involved in pathogenesis of ocular toxoplasmosis in mice. Infect Immun 1999;67:928-35.
[6] Vutova P, Wirth M, Hippe D, Gross U, Schulze-Osthoff K, Schmitz I, et al. Toxoplasma gondii inhibits Fas/CD95-triggered cell death by inducing aberrant processing and degradation of caspase 8. Cell Microbiol 2007;9:1556-70.
[7] Poissonnier A, Sanseau D, Le Gallo M, Malleter M, Levoin N, Viel R, et al. CD95-Mediated Calcium Signaling Promotes T Helper 17 Trafficking to Inflamed Organs in Lupus-Prone Mice. Immunity 2016;45:209-23.
[8] El-Taweel HA, Abou-Holw SA, Ghoniem HM. Alteration in circulating soluble Fas level in Toxoplasma seropositive pregnant women. J Egypt Soc Parasitol 2007;37:511-21.
[9] Guirelli PM, Angeloni MB, Barbosa BF, Gomes AO, Castro AS, Franco PS, et al. Trophoblast-macrophage crosstalk on human extravillous under Toxoplasma gondii infection. Placenta 2015;36:1106-14.
[10] Edwards-Smallbone J, Pleass RJ, Khan NA, Flynn RJ. Acanthamoeba interactions with the blood-brain barrier under dynamic fluid flow. Exp Parasitol 2012;132:367-72.
[11] Mishra BB, Gundra UM, Teale JM. STAT6(-)/(-) mice exhibit decreased cells with alternatively activated macrophage phenotypes and enhanced disease severity in murine neurocysticercosis. J Neuroimmunol 2011;232:26-34.
[12] Voehringer D, van Rooijen N, Locksley RM. Eosinophils develop in distinct stages and are recruited to peripheral sites by alternatively activated macrophages. J Leukoc Biol 2007;81:1434-44.
[13] Zhao A, Urban JF, Jr., Anthony RM, Sun R, Stiltz J, van Rooijen N, et al. Th2 cytokine-induced alterations in intestinal smooth muscle function depend on alternatively activated macrophages. Gastroenterology 2008;135:217-25 e1.
[14] Ho J, Pelzel C, Begitt A, Mee M, Elsheikha HM, Scott DJ, et al. STAT2 Is a Pervasive Cytokine Regulator due to Its Inhibition of STAT1 in Multiple Signaling Pathways. PLoS Biol 2016;14:e2000117.
[15] Butcher BA, Kim L, Panopoulos AD, Watowich SS, Murray PJ, Denkers EY. IL-10-independent STAT3 activation by Toxoplasma gondii mediates suppression of IL-12 and TNF-alpha in host macrophages. J Immunol 2005;174:3148-52.
[16] Portillo JC, Muniz-Feliciano L, Lopez Corcino Y, Lee SJ, Van Grol J, Parsons SJ, et al. Toxoplasma gondii induces FAK-Src-STAT3 signaling during infection of host cells that prevents parasite targeting by autophagy. PLoS Pathog 2017;13:e1006671.
[17] Jensen KD, Hu K, Whitmarsh RJ, Hassan MA, Julien L, Lu D, et al. Toxoplasma gondii rhoptry 16 kinase promotes host resistance to oral infection and intestinal inflammation only in the context of the dense granule protein GRA15. Infect Immun 2013;81:2156-67.

[18] Van Ginderachter JA, Beschin A, De Baetselier P, Raes G. Myeloid-derived suppressor cells in parasitic infections. Eur J Immunol 2010;40:2976-85.
[19] Dunay IR, Damatta RA, Fux B, Presti R, Greco S, Colonna M, et al. Gr1(+) inflammatory monocytes are required for mucosal resistance to the pathogen Toxoplasma gondii. Immunity 2008;29:306-17.
[20] Dunay IR, Sibley LD. Monocytes mediate mucosal immunity to Toxoplasma gondii. Curr Opin Immunol 2010;22:461-6.
[21] Robben PM, LaRegina M, Kuziel WA, Sibley LD. Recruitment of Gr-1+ monocytes is essential for control of acute toxoplasmosis. J Exp Med 2005;201:1761-9.
[22] Voisin MB, Buzoni-Gatel D, Bout D, Velge-Roussel F. Both expansion of regulatory GR1+ CD11b+ myeloid cells and anergy of T lymphocytes participate in hyporesponsiveness of the lung-associated immune system during acute toxoplasmosis. Infect Immun 2004;72:5487-92.
[23] Beaman MH, Hunter CA, Remington JS. Enhancement of intracellular replication of Toxoplasma gondii by IL-6. Interactions with IFN-gamma and TNF-alpha. J Immunol 1994;153:4583-7.
[24] Suzuki Y, Rani S, Liesenfeld O, Kojima T, Lim S, Nguyen TA, et al. Impaired resistance to the development of toxoplasmic encephalitis in interleukin-6-deficient mice. Infect Immun 1997;65:2339-45.
[25] Gordon S. Alternative activation of macrophages. Nat Rev Immunol 2003;3:23-35.
[26] Patil V, Zhao Y, Shah S, Fox BA, Rommereim LM, Bzik DJ, et al. Co-existence of classical and alternative activation programs in macrophages responding to Toxoplasma gondii. Int J Parasitol 2014;44:161-4.
[27] Fernando MR, Reyes JL, Iannuzzi J, Leung G, McKay DM. The pro-inflammatory cytokine, interleukin-6, enhances the polarization of alternatively activated macrophages. PLoS One 2014;9:e94188.
[28] Qualls JE, Neale G, Smith AM, Koo MS, DeFreitas AA, Zhang H, et al. Arginine usage in mycobacteria-infected macrophages depends on autocrine-paracrine cytokine signaling. Sci Signal 2010;3:ra62.
[29] Wu H, Zhen Y, Ma Z, Li H, Yu J, Xu ZG, et al. Arginase-1-dependent promotion of TH17 differentiation and disease progression by MDSCs in systemic lupus erythematosus. Sci Transl Med 2016;8:331ra40.

Figure Legends:

Figure 1: Cleaved-CD95L alters *T. gondii* replication within host cells. (A) VERO cells were either stimulated with doses of cl-CD95L as indicated. After 24 hours the cells were then infected with *T. gondii* at a MOI of 5 or left uninfected. After a further 48 hours post infection the percentage of monolayer was estimated for each group by examination under a light microscope. (**B)** VERO cells were either stimulated with 100ng/mL of cl-CD95L or left unstimulated. After 24 hours the cells were then infected with *T. gondii* at a MOI of 5 or left uninfected. After a further 48 hours post infection the parasite number was determined. **(C)** Supernatants from the above experiment were tested for ATP using Cell Titer-Glo. **(D)** Bone Marrow Derived Macrophages (BMDM) were either stimulated as in B). After 24 hours the BMDM (10^5) were then infected and parasite counts as in B). **(E)** As in D) but in the presence of Fas-Fc chimera (200ng/mL) or control antibody while undergoing cl-CD95L stimulation. All culture conditions were in triplicate and mean ±SD is shown with between 4-6 mice per experiment. With experiments repeated independently 6 times in A) or 5 times in B)-E). Data in (A), (C), and (E) were analysed by 2-way ANOVA and data in (B) and (D) by Unpaired T-tests; *P<0.05, **P<0.01, and ***P<0.0001.

Figure 2: cl-CD95L alters arginase-1 and IL-6 levels during *T. gondii* infection. A) BMDM (10^5 per well) were stimulated using indicated doses of cl-CD95L. After 24 hours the BMDM were then infected with *T. gondii* at a MOI of 5 or left uninfected. After a further 48 hours supernatants were assayed for IL -6 by ELISA. **B) – H)** BMDMs were treated with cl-CD95L at 100ng/mL or 0ng/mL control prior to infection with *T. gondii* at MOI 5. **B)** The addition of anti-IL-6 (120ng/mL) or control IgG was monitored for an effect on parasite counts as

393 performed in Figure 1. **C)** Arginase activity was measured 48hrs after infection cell lysates; **D)**
394 Inhibition of arginase was performed by addition of nor-NOHA (5mM) prior to measuring
395 parasite load; **E)** Matched cell lysates from B) were used to measure arginase activity after
396 anti-IL-6 treatment. STAT6 was inhibited (As1517499 – 0.2mg/mL) prior to infection and
397 during stimulation with cl-CD95L thereafter **F)** arginase activity was measured in cell lysates,
398 **G)** parasite numbers and **H)** IL-6 were measured in the supernatants. Treatments were
399 performed in triplicate and mean ±SD is shown with 4-6 mice per experiment. Each
400 experiment was repeats 5 times independently. Data was analysed in GraphPad Prism by 2-
401 way ANOVA where *P<0.05, **P<0.01, ***P<0.001, ****P<0.0001.

402 **Figure 3: cl-CD95L modifies the macrophage signalling landscape.** BMDM were treated with
403 100ng/mL of cl-CD95L for 24hrs prior to preparation for use in the Phospho-Kinase array
404 (R&D Systems). Pixel density captured in ImageJ was normalised to total protein levels. **A)**
405 Thereafter the Log_2 fold change in cl-CD95L stimulated vs unstimulated was calculated. The
406 blue dotted line indicates a Log_2 fold change while the red dotted line indicates a 2-Log_2 fold
407 change in expression levels. The 23 proteins with a Log^2 fold difference were then processed
408 in STRING V11.0 (string-db.org) program to identify potential interaction networks. B) The
409 top 5 biological processes and reactome pathways are identified presented. C) The potential
410 interaction network generated is presented, based upon known interactions taken from
411 InAct. The nature of the interaction is dictated as follows; lines with an arrowhead indicates
412 a positive interaction, lines with a rounded end indicate unknown interaction, lines with a
413 flat end indicate a negative end. Results shown are means from 2 independent biological
414 replicates for each treatment.

415

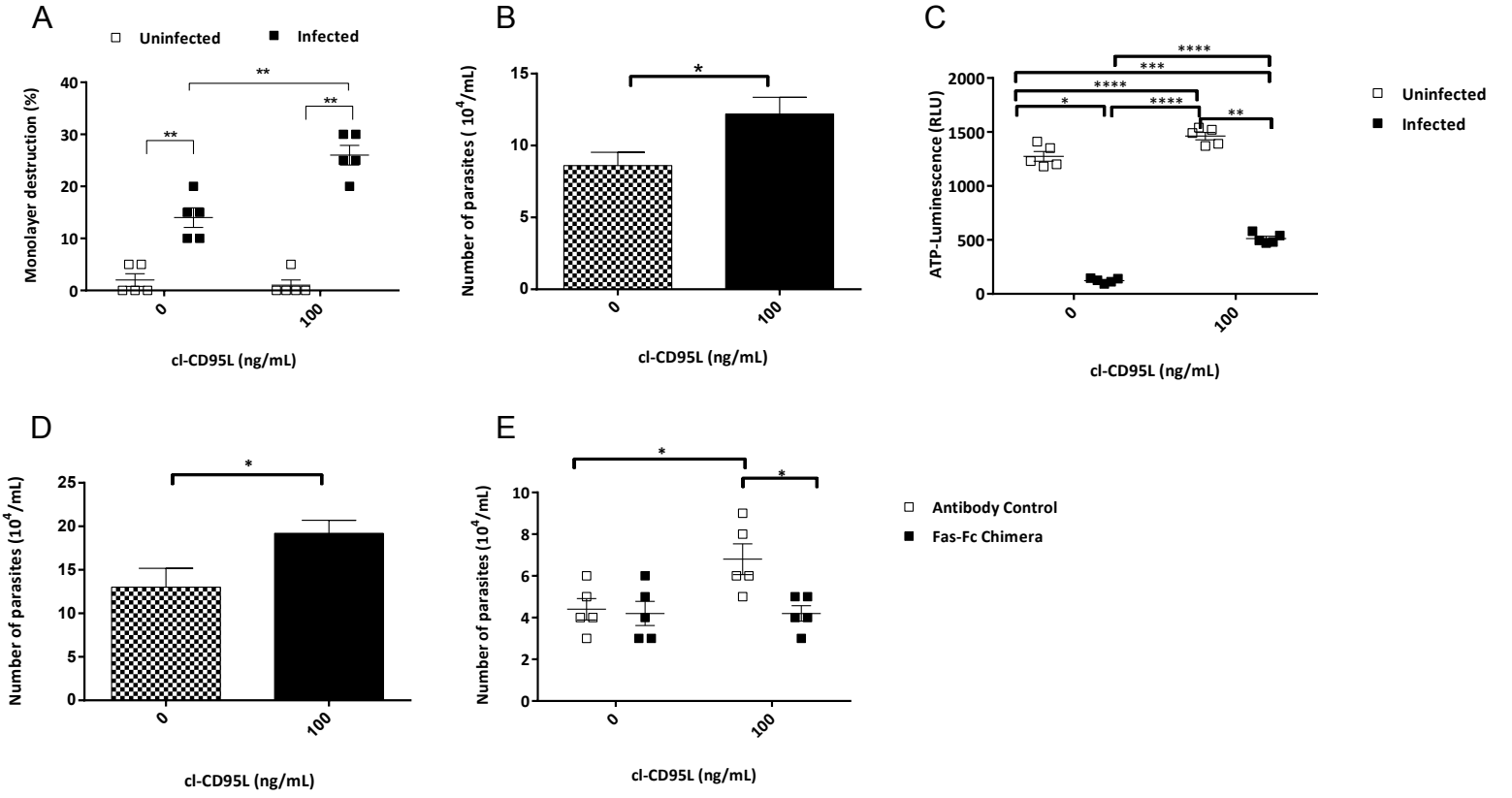
A
Uninfected
Infected
Monolayer destruction (%)
cl-CD95L (ng/mL)
B
Number of parasites (10^4/mL)
cl-CD95L (ng/mL)
C
ATP-Luminescence (RLU)
cl-CD95L (ng/mL)
Uninfected
Infected
D
Number of parasites (10^4/mL)
cl-CD95L (ng/mL)
E
Number of parasites (10^4/mL)
cl-CD95L (ng/mL)
Antibody Control
Fas-Fc Chimera

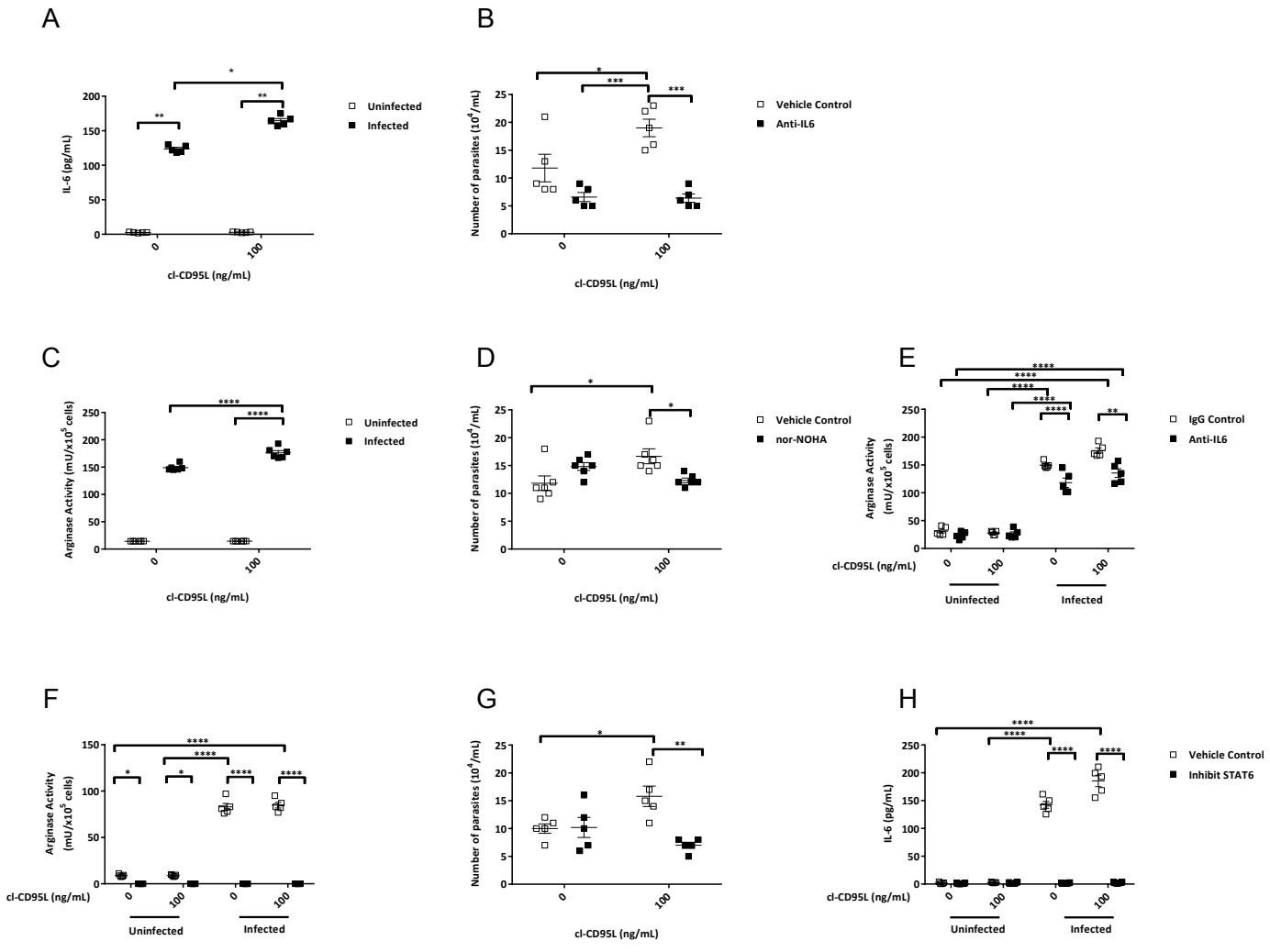
A
IL-6 (pg/mL)
cl-CD95L (ng/mL)
Uninfected
Infected
B
Number of parasites (10^6/mL)
cl-CD95L (ng/mL)
Vehicle Control
Anti-IL6
C
Arginase Activity (mU/x10^5 cells)
cl-CD95L (ng/mL)
Uninfected
Infected
D
Number of parasites (10^6/mL)
cl-CD95L (ng/mL)
Vehicle Control
nor-NOHA
E
Arginase Activity (mU/x10^5 cells)
cl-CD95L (ng/mL)
Uninfected
Infected
IgG Control
Anti-IL6
F
Arginase Activity (mU/x10^5 cells)
cl-CD95L (ng/mL)
Uninfected
Infected
G
Number of parasites (10^6/mL)
cl-CD95L (ng/mL)
H
IL-6 (pg/mL)
cl-CD95L (ng/mL)
Uninfected
Infected
Vehicle Control
Inhibit STAT6

A

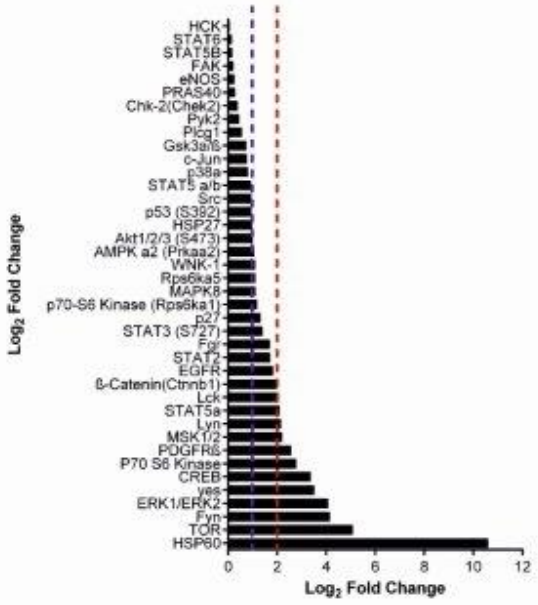

B

Biological Processes (GO)

GO-term	*Description*	*Count in network*
GO:0007165	signal transduction	40 of 3594
GO:0006468	protein phosphorylation	28 of 793
GO:0042981	regulation of apoptotic process	32 of 1476
GO:0016310	phosphorylation	29 of 1034
GO:0071310	cellular response to organic substance	33 of 1858

Reactome Pathways

Pathway	*Description*	*Count in network*
MMU-9006934	Signaling by Receptor Tyrosine Kinases	24 of 360
MMU-449147	Signaling by Interleukins	17 of 262
MMU-1280215	Cytokine Signaling in Immune system	18 of 357
MMU-168256	Immune System	26 of 1523
MMU-162582	Signal Transduction	30 of 2430

C